Proceedings of the ASME 2010 3rd Joint US-European Fluids Engineering Summer Meeting and 8th International Conference on Nanochannels, Microchannels, and Minichannels
FEDSM-ICNMM2010
August 1-5, 2010, Montreal, Canada

FEDSM-ICNMM2010-30223

FLUIDELASTIC INSTABILITY IN NORMAL AND PARALLEL TRIANGULAR ARRAYS OF FINNED TUBES

J. Wang
Department of Mechanical Engineering
McMaster University
Hamilton, Ontario, Canada, L8S4L7
Email:wangj73@mcmaster.ca

D.S. Weaver
Department of Mechanical Engineering
McMaster University
Hamilton, Ontario, Canada, L8S4L7
Email:weaverds@mcmaster.ca

ABSTRACT

An experimental study was carried out to investigate fluidelastic instability in finned tube bundles in normal and parallel triangular arrays. Three arrays of each geometry type were studied experimentally: two arrays with serrated, helically wound finned tubes of different fin densities, and a bare tube array with the same base diameter as the finned tubes. All six tube arrays studied had the same tube pitch.

The finned tubes under consideration were commercial finned tubes typically used in the fossil and process industries. For the purpose of the present investigation, the concept of "effective diameter" of a finned tube, as previously used to predict vortex shedding, was used to compare the finned tube results with other finned tube results as well as the existing bare tube world data.

The experimental results for the triangular arrays show that the fin's structure strongly influences the fluidelastic stability of finned tube bundles and the fin pitch is demonstrated to reduce the difference in the stability threshold between the tube array geometries as the fin density increases. Overall, the effect of serrated fins on fluidelastic instability is very complex and array geometry dependent, stabilizing some arrays and destabilizing others. Clearly, the effect of fins cannot be accounted for by the simple use of an effective diameter of an equivalent bare tube.

NOMENCLATURE

D	–	Characteristic length, diameter
D_b	–	Base or bare tube diameter
D_{eff}	–	Effective tube diameter
D_f	–	Fin diameter
D_{vol}	–	Volume based effective diameter
f	–	Natural frequency of the tube
G, g	–	Strain gage or gap
h	–	Fin height
h_s	–	Fin serration height
m	–	Tube mass per unit length
p	–	Fin pitch
P	–	Tube pitch
P/D_{eff}	–	Effective pitch ratio
t	–	Fin thickness
U_{crit}	–	Critical velocity
U_g	–	Gap velocity
U_u	–	Upstream velocity
w	–	Fin serration width
x	–	X direction
y	–	Y direction or amplitude
δ	–	Logarithmic decrement of damping
ζ	–	Damping factor, $\zeta=\delta/2\pi$
ρ	–	Fluid density

INTRODUCTION

A significant cause of tube failures in modern tube and shell heat exchangers is flow-induced vibrations. Of the various flow excitation mechanisms, turbulence can cause long term fretting wear at the tubes supports while vortex shedding can cause excessive noise levels through acoustic resonance in the shell cavity. However, by far the most potentially damaging mechanism is fluidelastic instability which can cause massive tube failures in a matter of hours [1]. Much research has been conducted over the past 40 years so that a reasonable understanding of the excitation mechanisms as well as predictive methodologies have been developed. Excellent reviews and design guidelines have been presented by Païdoussis [2], Weaver and Fitzpatrick [3], Pettigrew and Taylor [4], and Schröder and Gelbe [5].

Much of the research in this field has been driven by the nuclear industry, especially related to nuclear steam generators. These steam generators typically use small diameter tubes and relatively small pitch ratios and the vast majority of the published literature are related to such equipment. On the other hand, the chemical process and fossil industries tend to use much larger diameter tubes and larger pitch ratios. Moreover, these industries sometimes use heat transfer enhancing tubes such as "platen fin" tube assemblies [6] and spirally wound finned tubes [7], although the published literature relating to fluid-induced vibrations in finned tubes is very sparse.

As finned tubes have gained wider use for their enhanced heat transfer characteristics, researchers have sought to develop an "effective diameter" concept which was intended to allow the performance of finned tubes to be compared to that of bare tubes. If this idea should prove to be valid, this might permit the vast data available for bare tubes to be used for predicting the performance of finned tubes.

Mair et al [8] studied vortex shedding in finned tube arrays and proposed an effective diameter, D_{eff}, based on the projected frontal area of the tube and fins where D_f is the fin diameter, D_b is the bare tube diameter, t is the fin thickness, and p is the fin pitch.

$$D_{eff} = D_b + \frac{t(D_f - D_b)}{p} \qquad (1)$$

Halle et al [9] apparently used a volumetrically based effective diameter but did not publish their equation. However, Hirota et al [10] also proposed an effective diameter based on fin volume, distinguished here using D_{vol}.

$$D_{vol} = \sqrt{\left(D_f^2 - D_b^2\right)\frac{t}{p} + D_b^2} \qquad (2)$$

It should be noted that these approaches are both based on plain fins with no serrations or twists as are used in the present study. Additionally, use of these 'effective diameters' implicitly assumes that the effects of fins can be accounted for simply by augmenting the diameter of a bare tube. Interestingly, Mair et al showed that the use of their effective diameter was successful when comparing the results for vortex shedding from plain finned tubes and bare tubes. More recently, Ryu et al [11] and Jebodhsingh et al [12] studied vortex shedding from serrated finned tubes arrays and found similar results. The use of Mair et al's effective diameter proved to be a useful predictor for vortex shedding from these finned tubes.

Studies relating to fluidelastic instability in finned tube bundles are rare. Kienböck [13] and Halle et al. [9] conducted investigations into this issue but the finned tubes used had very short fins compared to their diameter ($h/D_b=6.6\%$ and 10% respectively, where h is the fin height). The most recently published paper, by Lumsden and Weaver [7], considers an array of industrial serrated finned tubes with much larger fin height, $h/D_b=50\%$. The experiments were conducted to study fluidelastic instability in in-line and rotated square finned tube arrays. Coarse finned tubes, fine finned tubes, and bare tubes were considered (their detail dimensions will be introduced in the following section). For these finned tubes, the effective diameter computed using equations (1) and (2) gave results which were only *4-6%* different. Thus, they used the Mair et al definition for effective diameter to normalize their data. The tube pitch and mass ratio were kept constant. Lumsden and Weaver showed for the first time that fluidelastic instability could occur in in-line and rotated square arrays of serrated finned tubes. They compared their results to the world data and found that, for in-line square arrays, the finned tubes had a much higher critical reduced velocity than the bare tubes, i.e., the fins appeared to have a stabilizing effect. However, the results for the rotated square array showed the opposite trend, a destabilizing effect of fins. This might, at least in part, be accounted for by the reduction in effective pitch ratio caused by the addition of the fins. The Lumsden and Weaver investigation suggests that the effect of fins on fluidelastic instability is strongly dependent on tube array geometry and that more research is required to determine the effects of tube array pitch and pattern.

The purpose of this paper is to present the results of an experimental study of fluidelastic instability in parallel and normal triangular arrays of serrated finned tubes, for which no previous results have been published. In all, six different cases were studied; finely pitched and coarsely pitched serrated finned tubes and a datum case of bare tubes for each of the triangular array geometries. The results are compared with world data for finned and bare tube arrays.

APPARATUS AND EXPERIMENTS

Finned tubes geometry

The two kinds of steel finned tubes under investigation in this study were manufactured by Biraghi Canada (a subsidiary of Fintube Corp. and are shown in Fig. 1. These are the same finned tubes as used in the experiments of Lumsden and Weaver[7]. The fin pitch of the coarse finned tube and fine finned tube are 8.4mm (3.3 fins per inch) and 4.2mm (5.7 fins per inch) respectively. As a reference, a bare tube with the same base diameter (38.4mm) as the finned tubes was also studied.

a) Coarse finned tube (8.4mm or 3.3 fpi)

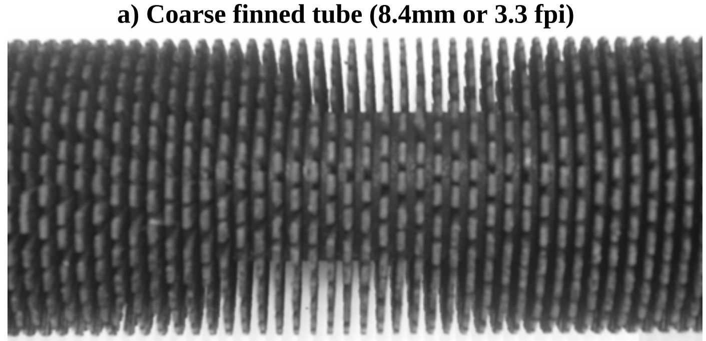

b) Fine finned tube (4.2mm or 5.7 fpi)

Fig. 1 Photos of finned tubes

The tube arrangement studied consists of a tube with a threaded rod support at one end and a steel cap at the other end. The threaded rod is used to fix the tube into the base plate of the test section as seen in Fig. 2. The rod length is one of two adjustable parameters (the other is added end mass) used to tune the tube to the desired natural frequency. In addition, the slender rod will reduce the effective stiffness of the tested tube to better simulate the natural frequencies of the much longer tubes used in service. The steel cap is applied to provide added end mass for the bare tube and the coarse finned tube to help maintain dynamic similarity of the experiments which will be discussed further below. The detailed geometries of the serrated, helically wound fins are shown in Table 1 where h is the overall fin height, w is the serration width, h_s is the serration height, and t is the fin thickness.

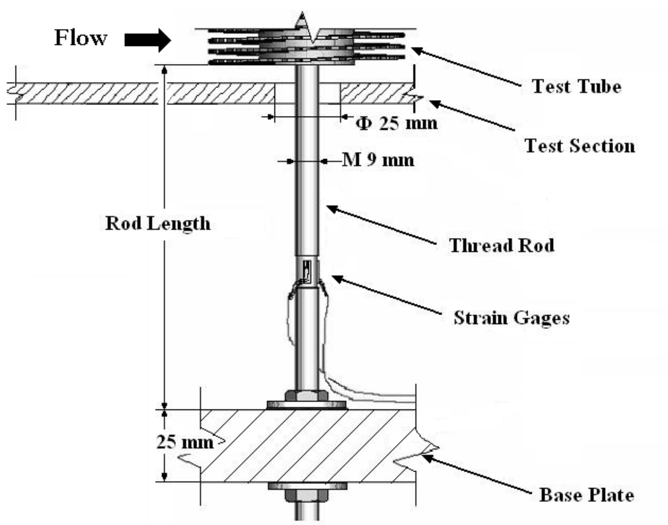

Fig. 2 Test tube support, monitored tubes

Table 1 Fin geometries mm (inch)

tube	h	w	h_s	t
3.3fpi	18.5(0.728)	4.4(0.173)	12.7(0.5)	1.3(0.051)
5.7fpi	19.1(0.752)	4.5(0.177)	12.7(0.5)	1.3(0.051)

Triangular arrays

Two types of triangular geometries are examined, normal triangular arrays and parallel triangular arrays as shown in Fig. 3. Since the arrangements affect the dimensions of the test section, the positions of tubes in both transverse and streamwise directions must be carefully designed to fit all the tubes into the wind tunnel test section which is 686mm in length (streamwise), 618mm in width and 616mm in height.

As the normal triangular array can be rotated 90 degrees to become a parallel triangular array, the base plate on which all the tubes are mounted need only be designed for a single equilateral triangular pattern of tubes. For practical reasons, the tube pitch was kept constant at 89.2mm for all the arrays studied. The base plate structure consists basically of a 25.4mm thick steel plate drilled through for the support rods as seen in Fig. 2. The accuracy of tube pitch depends on the position accuracy and diameter size of each hole drilled in the base plate, which was carried out using a CNC machine with a precision of ±0.425mm. Compared to the 89.2mm tube pitch, the relative error is ±0.5%. The test section has a square cross section of 0.618×0.616m^2. The normal triangular arrays (see Fig. 3-a) consist of 32 flexible tubes, and the parallel triangular arrays (see Fig. 3-b) consist of 24 flexible tubes. Half tubes are used as the boundaries of the test section on both sides. The test section was designed to be adjustable for the different tube types and array geometries. The specifications for the triangular arrays are given in Table 2.

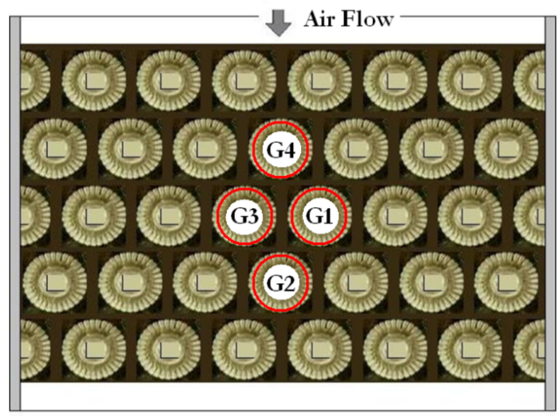

a) Normal triangular array

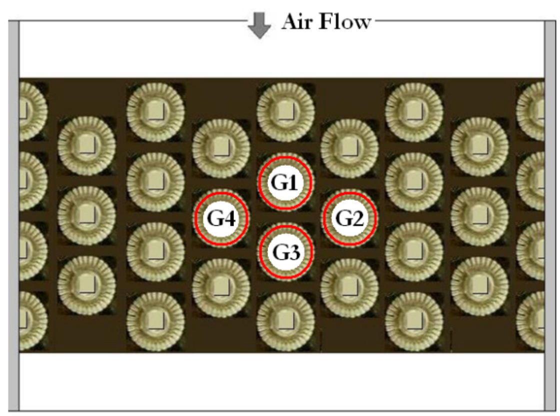

b) Parallel triangular array
Fig. 3 Triangular arrangements

Table 2 Specifications of triangular arrays

P *(mm)*	D_{eff} *(mm)*			P/D_{eff}		
	bare tube	3.3fpi	5.7fpi	bare tube	3.3fpi	5.7fpi
89.2	38.4	44.4	51.5	2.32	2.01	1.73

Dynamic similarity

The dynamic similarity between the fine finned tube array and coarse finned tube array is maintained through the mass ratio and the natural frequency of tubes. The mass ratio is defined as $m/\rho D^2_{eff}$. Since the mass ratio of the coarse finned tubes should be as close as possible to the mass ratio of the fine finned tubes and the mass of the fine finned tubes is greater than that of the coarse finned tubes , an end mass was added to the coarse finned tubes. The natural frequencies for all of the tubes of each type should ideally be tuned to be the same for the experiments. The tube frequency is determined primarily by the rod length and tube mass. When the tube mass (including the added end mass, if any) has been determined, the rod length will be the only factor affecting the natural frequency of tube. A complicating factor is that the rod length determines the distance between the base plate and the wind tunnel the test section, which then affects other assemblies and the supporting structure. Therefore, the rod length must be carefully determined to set the desired natural frequency range of the tubes. In the end, practicality dictated that dynamic similarity between the various arrays could only be satisfied approximately. The bare tubes were a particular problem because sufficient support rod length and/or end mass could not be achieved to obtain a match of natural frequency or mass ratio with the finned tubes. The mass data used is listed in Table 3. The total mass of the normal triangular tube bundle and support assembly was over 350 kg and the whole assembly was fastened directly to the laboratory floor.

Table 3 Mass parameters of tubes

	net tube mass (kg)	end mass (kg)	m (kg/m)	mass ratio
bare tube	2.46	0.42	4.06	2340
3.3fpi	3.86	0.10	6.35	2740
5.7fpi	5.06	0	8.31	2660

Displacement measurement

The tubes were 608mm in length, just short of the 616mm height of the test section, with a threaded support rod welded to the bottom of each tube in a cantilever fashion. Four tubes are monitored in each array using two strain gages attached to the support rod, one in each of the streamwise and transverse flow directions, to capture their respective amplitudes of vibration. The positions and numbers of the four monitored tubes are shown as Fig. 3, while the strain gages are shown schematically in Fig. 2. The support rods are fixed to the base plate with a nut and washer above and below the plate, and all nuts were torqued to the pre-load of about 20 Nm.

The displacement of the top end of the tube from its stationary position defines the tube amplitude. The calibration was conducted after the assembled and tuned test section was set into the wind tunnel. The resulting voltage-displacement relationships were linear and used to interpret the strain gage output voltage signal in terms of displacement amplitudes during the experiments. The actual displacements presented are the vector magnitudes of the streamwise and transverse signals. Thus, the amplitudes quoted and plotted in this paper are obtained by computing the square root of the sum of squares of the measured response for each of the streamwise and transverse directions of a monitored tube. As seen in Fig. 2, the monitored tubes are designated G1 to G4, inclusive.

Damping and natural frequency

The tube damping was obtained by plucking the tubes and recording their transient response. The peaks of the decaying vibration signal can be used to compute the logarithmic decrement of damping directly, or an exponential fit of the decay curve can be used to determine the damping coefficient. The natural frequency and vibration amplitude were obtained from the Fast Fourier Transform (FFT) of the vibration signals. The FFT was obtained using an HP 35670A analyzer as well as the mathematical software Origin, depending on convenience and the need for post-processing in the particular experiment.

The natural frequency and damping data from the four monitored tubes is summarized in Table 4. It is seen that the four monitored tube natural frequencies for each of the three different tube arrangements are the same within *1%* of their mean value. It is also seen that the damping is very light and somewhat more variable. Additionally, the damping increases monotonically with the addition of fins and increasing fin density. It seems likely that this is the result of the increasing aerodynamic component of damping.

Table 4 Natural frequency and damping of tube

tubes	Natural frequency *f(Hz)*			Logarithmic decrement of damping δ		
	bare tube	3.3fpi	5.7fpi	bare tube	3.3fpi	5.7fpi
G1	4.25	2.49	2.48	0.0029	0.0056	0.0084
G2	4.25	2.50	2.50	0.0033	0.0050	0.0066
G3	4.24	2.50	2.47	0.0034	0.0057	0.0074
G4	4.29	2.51	2.46	0.0027	0.0060	0.0077
mean	4.26	2.50	2.48	0.0031	0.0056	0.0075

Tuning non-instrumented tubes

All of the non-instrumented tubes in each of the arrays were also tuned to the frequency of the monitored tubes using an accelerometer. The accelerometer signals were analyzed using the HP analyzer to obtain the tube natural frequency. If the frequency was not equal to the desired value, the support rod length was adjusted and the testing repeated until frequency coincidence was achieved within a relative error of ±*1%*.

Experimental procedure

The experiments were conducted in the low speed wind tunnel, with turbulence upstream of the test section below *1%*. Velocity measurements were obtained using a pitot probe upstream of the test section, together with a Betz micromanometer. Calibration of the Betz indicated a maximum error in velocity of about *2.5%*. The upstream velocity was converted to mean gap velocity using equation (3).

$$U_g = U_u \frac{P}{P - D_{eff}} \qquad (3)$$

where U_g is the mean gap velocity between the tubes, U_u is the velocity measured upstream, P is the tube pitch, D_{eff} is the effective tube diameter.

The procedure was the same for all of the bundles studied. The wind tunnel velocity was set at some desired value and measurements commenced after a time period sufficient for the system to reach a steady state response (typically 8-10 minutes). The velocity was determined using the pitot probe and Betz micromanometer, and the tube response for each of the monitored tubes recorded using the HP analyzer. This response data was stored on a floppy disc and used to compute frequency and overall response records after completion of an experimental run.

Once these measurements were complete, the flow velocity was incremented and the measurements repeated until the experiment was terminated. Each run was considered complete when there was either fin-to-fin impacting in the cases for finned tubes, or there was danger that larger response amplitudes might produce plastic deformation of the tube support rods in the cases of bare tubes.

RESULTS AND DISCUSSIONS

Experimental results

The results for the parallel triangular arrays are presented in Figs. 4(a-c) inclusive. These plots are the overall Root of Mean Square (RMS) *amplitude/*D_{eff} versus reduced gap velocity (U_g/fD_{eff}). In both parameters, the "effective diameter" has been used for normalization as stated above. The legends in the figures showing G1 to G4 inclusive refer to the data from the four monitored tubes as shown in Fig. 3. In some cases, experiments were repeated and the data are shown by a hyphen and experiment number. Thus, G3-2, for example, represents the results for the second experimental run for tube G3.

Fig. 4(a) shows the typical flow induced response behavior for bundles of bare tubes in gas cross-flow. All four of the monitored tubes change abruptly from small amplitude random turbulence excited response to large amplitude periodic response at a reduced velocity of about 25. This is taken as the fluidelastic stability threshold and is very clearly defined.

Fig. 4(b) shows the results for the parallel triangular array of coarse finned tubes (8.4mm or 3.3fpi). The stability threshold is reasonably well defined at a reduced velocity of about 53, more than twice that for the bare tube array. However, the post-stable response is rather complex. Visual observations indicate that tube-to-tube clashing occurs followed by a rapid reduction in tube amplitudes. Vibration amplitudes vary from tube to tube and, overall, the tubes response is highly modulated. Repeated experiments confirmed this behavior and a critical reduced velocity of about 53.

Fig. 4(c) shows the dynamic responses of the fine finned tubes (4.2mm or 5.7fpi) for the parallel triangular array as a function of reduced flow velocity. The critical reduced velocity is reasonably well defined and taken to be about 46, a little less than that for the coarse finned tube array. The range of critical reduced velocity is from 43~49, the average value being approximately 46.

Figs. 4(d-f) provide the results for the normal triangular arrays. The bare tube results in Fig. 4(d) indicate some variability between tubes and between different runs with a threshold reduced velocity ranging approximately from 55 to 61, the average value being taken as about 58. As expected, this is about double that for the parallel triangular array of bare tubes.

Interestingly, Fig. 4(e) shows that the coarse finned tube array has a more clearly defined stability threshold than the bare tube array, but a somewhat higher critical reduced velocity of about 72. Fig. 4(f) provides the results for the fine finned tube array and shows a well defined critical reduced velocity of about 43. It is noteworthy that this is even less than for the bare tube array. At least in part, this may be attributable to the much smaller pitch ratio based on effective tube diameter.

The critical reduced velocity and associated mass-damping parameters for each of the arrays are listed in Table 5.

Table 5 Critical reduced velocity vs. damping parameter

	parallel array		normal array	
	reduced velocity (U_g/fD_{eff})	mass damping parameter ($m\delta/\rho D^2_{eff}$)	reduced velocity (U_g/fD_{eff})	mass damping parameter ($m\delta/\rho D^2_{eff}$)
bare tube	25	7.13	55-61	7.13
3.3fpi	53	15.33	73	15.33
5.7fpi	46	20.02	43	20.02

Discussions

The experimental results for each array geometry are compared with the world data on the Weaver and Fitzpatrick [3] stability maps for parallel and normal triangular arrays in Figs. 5 and 6, respectively. All of the present data falls near or above the world data for the arrays tested. This is thought to be due largely to the very large pitch ratio of the present arrays in comparison with those of the vast majority of the other data plotted, which has small pitch ratios typical of nuclear steam generators. The nuclear industry has driven much of the research in this field, especially in relation to nuclear steam generators which typically have pitch ratios less than *1.5*. The fossil fuel industry typically employs much larger pitch ratios and the present study employs commercial finned tubes typical of that industry.

Fig. 5 shows that the critical reduced velocity for both the fine and coarse finned parallel triangular tube arrays are well above the world data as well as for the bare tube datum for the present study. Apparently, serrated fins have a stabilizing effect on parallel triangular tube arrays, at least for the arrays studied.

The results for the normal triangular arrays are more complex as seen in Fig. 6. The coarse finned array has a critical reduced velocity higher than that for the bare tube array but the fine finned array has a critical velocity substantially below both the coarse finned and bare tube arrays. Thus, fine serrated fins apparently have a destabilizing effect on normal triangular arrays, contrary to the effect observed for parallel triangular arrays.

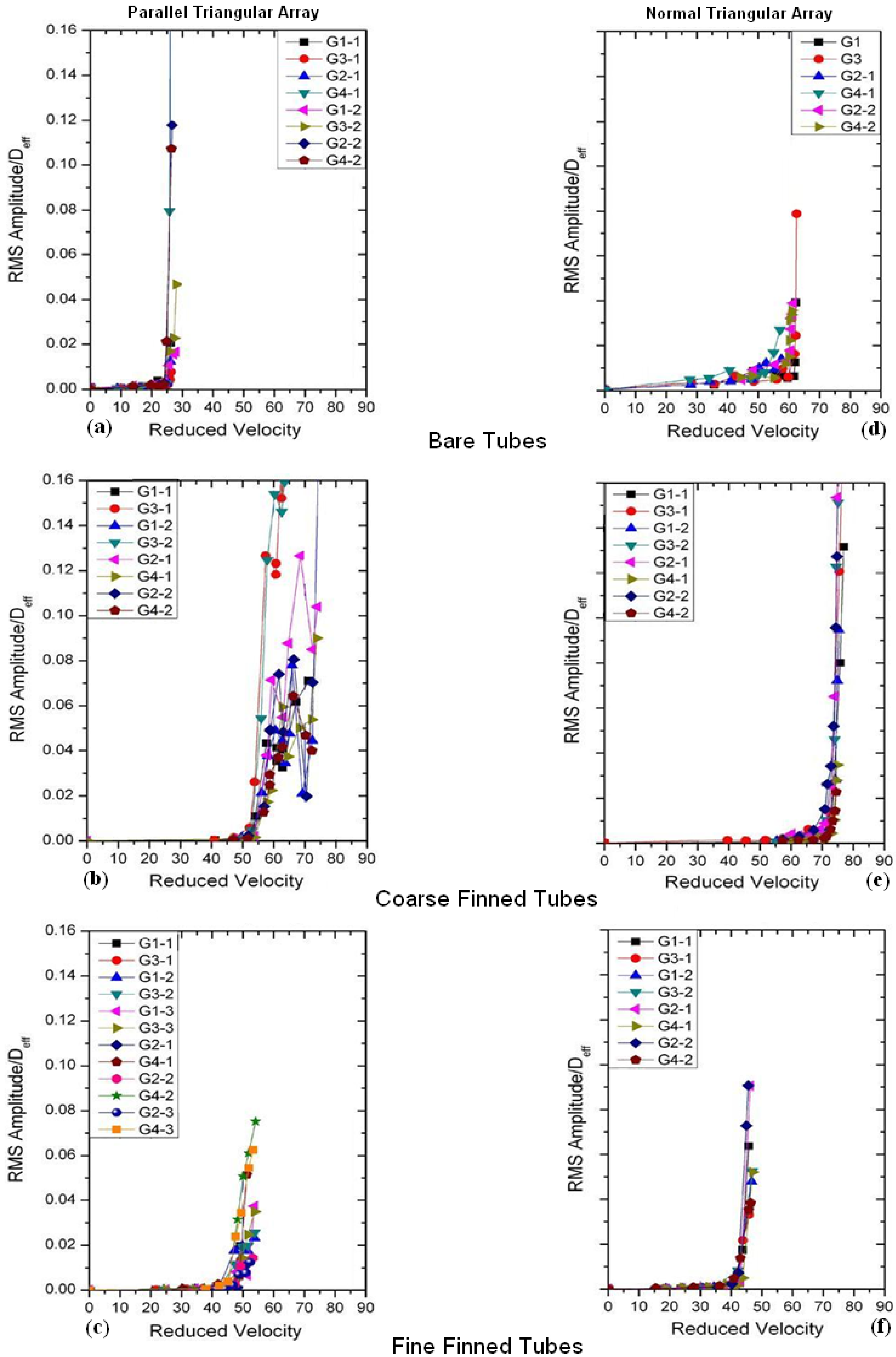

Fig. 4 RMS amplitude/D_{eff} v.s. reduced velocity

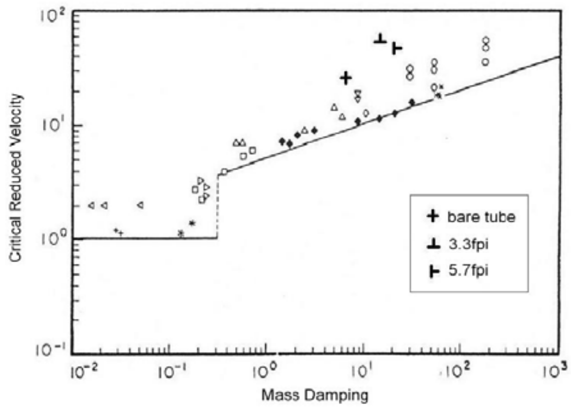

Fig. 5 Parallel triangular arrays in world data

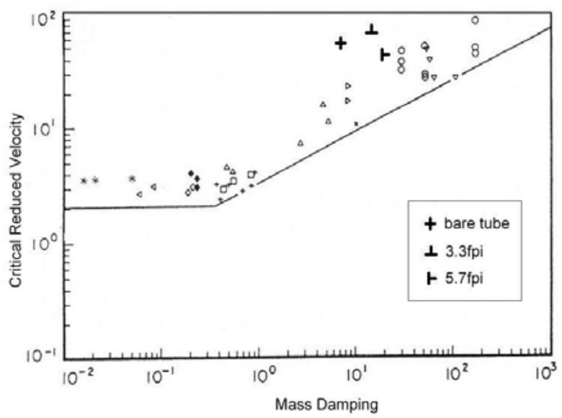

Fig. 6 Normal triangular arrays in world data

It is instructive to plot the critical reduced velocity against the pitch ratio for the present arrays together with those studied by Lumsden and Weaver [7] who used the same tubing. Fig. 7 shows the bare tube grouping denoted by "A", representing the datum case. The critical velocities for the normal triangular and rotated square tubes arrays are close together and much higher than those for the parallel triangular and inline square arrays, as expected. Interestingly, the results for all array geometries are relatively close together for the fine finned tubes which have the smallest pitch ratio based on effective diameter. Thus, the effect of finely spaced serrated fins is to stabilize parallel triangular and inline square tube arrays, and to destabilize normal triangular and rotated square arrays when compared to the bare tube datum cases. The effects of coarse fins on array stability are not so clear. Both triangular arrays are stabilized over their bare tube datum case by coarse fins but both are then destabilized with fine fins as compared with their respective coarse fin results. The inline and rotated square arrays show opposite trends from one another. While this behavior is not understood, it is clear that the effects of fins on tubes cannot be simply accounted for by the use of an "effective diameter" in the standard parameters used to define fluidelastic stability behavior in tube arrays. Logically, a tube with very coarse (widely spaced) fins should behave like a bare tube while a tube with very finely spaced fins should behave more like a bare tube with a diameter equal to the fin diameter. In between these extremes, the results show that the effects of fins are very dependent on the array geometry and may be stabilizing or destabilizing. This result is in stark contrast to that for vortex shedding from finned tubes which seems to be reasonably well accounted for using the concept of an effective bare tube diameter. More basic research is required to develop an understanding of this behavior.

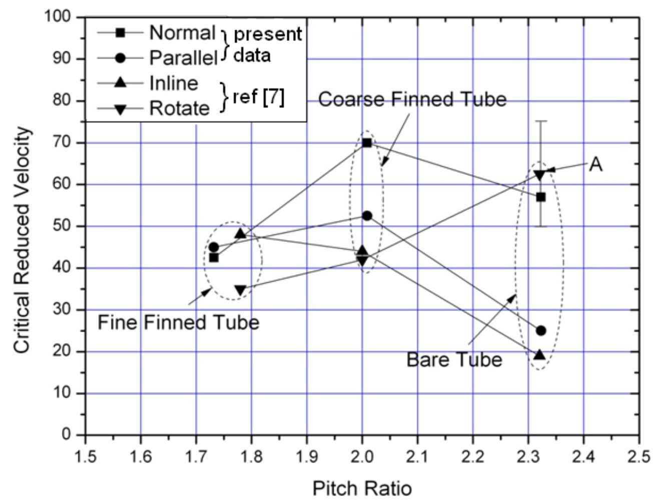

Fig. 7 Critical reduced velocity vs. pitch ratio

CONCLUSIONS

Wind tunnel experiments were conducted to study fluidelastic instability in normal and parallel triangular arrays of serrated finned tubes. For each tube array geometry, fine finned (4.2mm/5.7fpi) and coarse finned (8.4mm/3.3fpi) tubes were considered as well as bare tubes as a datum case. The results were compared with world data as well as the only existing data for fluidelastic instability in finned tube arrays. The principal conclusions drawn are:

1. The critical velocities in normal and parallel triangular tube arrays are substantially delayed by the addition of coarse serrated fins, even though the addition of the fins reduces the tube pitch ratio based on the effective diameter. These fins have a stabilizing effect on fluidelastic stability.

2. An increase in fin density from the coarse fin case to the fine fin case has an apparent destabilizing effect, perhaps partially accounted for by the reduction in pitch ratio based on effective tube diameter.

3. While an "effective diameter" may be useful as a normalizing parameter for comparing fluidelastic stability data for finned tube arrays to that for bare tube arrays, it is clear that the effects of fins on tube array stability is strongly dependent on array geometry and cannot be accounted for simply through the concept of an equivalent bare tube.

ACKNOWLEDGMENTS

The authors gratefully acknowledge the financial support of The Natural Sciences and Engineering Research Council of Canada (NSERC) and Frank Eisinger & Foster Wheeler Power Group, Inc. for supplying the tubes for this study.

REFERENCES

1) Yu, X., "An analysis of tube failure in a U-shape tube bundle", *Flow Induced Vibration-1986*, Chen, S.S., Simonis, J.C., Shin, Y.S., eds., ASME PVP-Vol. 104, pp. 187-192, 1986.
2) Païdoussis, M.P., "A review of flow-induced vibrations in reactors and reactor components", *Nuclear Engineering and Design*, 74, pp. 31-60, 1982.
3) Weaver, D.S. and Fitzpatrick, J.A., "A review of cross flow induced vibrations in heat exchanger tube arrays", *Journal of Fluids and Structures*, (2), 73-93, 1988.
4) Pettigrew, M.J. and Taylor, C.E., "Vibration analysis of shell and tube heat exchangers: An overview -Part 1: Flow damping, fluidelastic instability -Part 2: Vibration response, fretting wear, guidelines", *Journal of Fluids and Structures*, 18, pp469-500, 2003.
5) Schröder, K. and Gelbe, H., "New design recommendations for fluidelastic instability in heat exchanger tube bundles". *Journal of Fluids and Structures*, 18, pp 361-379, 1999.
6) Weaver, D.S., Ziada, S., Sun, Z., Feenstra, P., "The effect of platen fins on the flow-induced vibrations of an in-line tube array", *ASME J. Pressure Vessel Technology,* Vol. 123(4), pp. 437-441, 2001.
7) Lumsden, R.H. and Weaver, D.S., "The effect of fins on fluidelastic instability in in-line and rotated square arrays", *ASME PVP FSI,* Vol 4, M. Moatamedi ed., San Antonio, TX, PVP 2007-26597, pp.465-473, 2007. (to appear in JPVT, 2010)
8) Mair, W.A., Jones, P.D.F. and Palmer, R.K.W., "Vortex shedding from finned tubes". *Journal of Sound and Vibration*, 39(3), pp. 293-296, 1975.
9) Halle, H., Chenoweth, J.M. and Wambsganss, M.W., "Flow-induced tube vibration thresholds in heat exchangers from shell side water tests". *ASME Symposium on Flow-Induced Vibrations*, Vol. 3, New Orleans, pp. 17-32. 1984.
10) Hirota, K., Nakamura, T., Kikuchi, H., Isozaki, K. and Kawahara, H., "Fluid elastic and vortex induced vibration of a finned tube array", *ASME Proceedings of IMECE2002*, New Orleans, Paper No. 32793, 2002.
11) Ryu, B.N., Kim, K.C. and Boo, J.S., "The effect of serrated fins on the flow around a circular cylinder", *KSME International Journal*, 17(6), pp.925-934, 2003.
12) Ziada, S., Jebodhsingh, D., Weaver, D.S., and Eisinger, F.L., "The Effect of Fins on Vortex Shedding fron a Cylinder in Cross-Flow", *Journal of Fluids and Structures*, Vol 21, pp. 65-74, 2005.
13) Kienböck, M., "Vibration characteristics of finned tubes with small fins". *VGB Kraftwerkstechnik*, 62(7), pp. 498-506, English translation, 1982.

